Citation: Cell Death and Disease (2012) 3, e302; doi:10.1038/cddis.2012.36

www.nature.com/cddis

TIAF1 self-aggregation in peritumor capsule formation, spontaneous activation of SMAD-responsive promoter in p53-deficient environment, and cell death

J-Y Chang[1], M-F Chiang[2], S-R Lin[1], M-H Lee[1], H He[1], P-Y Chou[1], S-J Chen[1], Y-A Chen[1], L-Y Yang[1], F-J Lai[3], C-C Hsieh[3], T-H Hsieh[4], H-M Sheu[5], C-I Sze[4] and N-S Chang*[,1,2,6,7,8]

Self-aggregation of transforming growth factor β (TGF-β)1-induced antiapoptotic factor (TIAF1) is known in the nondemented human hippocampus, and the aggregating process may lead to generation of amyloid β (Aβ) for causing neurodegeneration. Here, we determined that overexpressed TIAF1 exhibits as aggregates together with Smad4 and Aβ in the cancer stroma and peritumor capsules of solid tumors. Also, TIAF1/Aβ aggregates are shown on the interface between brain neural cells and the metastatic cancer cell mass. TIAF1 is upregulated in developing tumors, but may disappear in established metastatic cancer cells. Growing neuroblastoma cells on the extracellular matrices from other cancer cell types induced production of aggregated TIAF1 and Aβ. *In vitro* induction of TIAF1 self-association upregulated the expression of tumor suppressors Smad4 and WW domain-containing oxidoreductase (WOX1 or WWOX), and WOX1 in turn increased the TIAF1 expression. TIAF1/Smad4 interaction further enhanced Aβ formation. TIAF1 is known to suppress SMAD-regulated promoter activation. Intriguingly, without p53, self-aggregating TIAF1 spontaneously activated the SMAD-regulated promoter. TIAF1 was essential for p53-, WOX1- and dominant-negative JNK1-induced cell death. TIAF1, p53 and WOX1 acted synergistically in suppressing anchorage-independent growth, blocking cell migration and causing apoptosis. Together, TIAF1 shows an aggregation-dependent control of tumor progression and metastasis, and regulation of cell death.

Cell Death and Disease (2012) **3,** e302; doi:10.1038/cddis.2012.36; published online 26 April 2012
Subject Category: Experimental Medicine

Transforming growth factor β (TGF-β) family proteins participate in a variety of biological events and diseases, including cell proliferation, immune response, apoptosis, oncogenesis and many physiological events.[1,2] TGF-β has dual roles in cancer initiation and progression.[3,4] TGF-β inhibits epithelial cell growth, and induces epithelial to mesenchymal transition (EMT). Cancerous cells are refractory to TGF-β-mediated growth suppression, and produce autocrine TGF-β for their growth and metastasis. The mechanism of this regard is largely unknown.

TGF-β1-induced antiapoptotic factor (TIAF1) is a 12-kDa TGF-β1-induced antiapoptotic factor, which protects murine L929 fibroblasts from apoptosis by tumor necrosis factor (TNF) and overexpressed TNF receptor adaptor proteins in the presence of actinomycin D, an inhibitor of DNA transcription.[5,6] Transiently overexpressed TIAF1 supports fibroblast growth, which is similar to the effect of TGF-β1.[6] Also, like TGF-β1, ectopic TIAF1 suppresses cell growth and induces apoptosis of monocytic U937 and many non-fibroblast cells.[6] TIAF1 increases the expression of p53 and Cip1/p21 and suppresses ERK phosphorylation in U937 cells, thereby inhibiting cell growth and inducing apoptosis.[6] Ectopic TIAF1 upregulates the expression of tumor suppressor p53, and both proteins mediate cell death in either a cooperative or an antagonistic manner.[7] Suppression of TIAF1 expression by small interfering RNA (siRNA) prevents UV irradiation-mediated p53 phosphorylation and nuclear translocation.

Expression of TIAF1 is significantly increased in activated helper T lymphocytes (TH2) in patients with chronic kidney and liver allograft rejection.[8] Regulatory T cells (Treg) have a significantly increased expression of TIAF1.[9] Whether TIAF1 controls the differentiation and activation-induced death of

[1]Institute of Molecular Medicine, National Cheng Kung University College of Medicine, Tainan, Taiwan, ROC; [2]Department of Neurosurgery, Mackay Memorial Hospital, Graduate Institute of Injury Prevention and Control, Taipei Medical University, Taipei, Taiwan, ROC; [3]Department of Dermatology, Chi-Mei Medical Center, Tainan, Taiwan, ROC; [4]Department of Anatomy and Cell Biology, National Cheng Kung University College of Medicine, Tainan, Taiwan, ROC; [5]Department of Dermatology, National Cheng Kung University College of Medicine, Tainan, Taiwan, ROC; [6]Advanced Optoelectronic Technology Center, National Cheng Kung University College of Medicine, Tainan, Taiwan, ROC; [7]Center of Infectious Disease and Signal Research, National Cheng Kung University, Tainan, Taiwan, ROC and [8]Department of Neuroscience and Physiology, SUNY Upstate Medical University, Syracuse, NY, USA
*Corresponding authors: N-S Chang, Institute of Molecular Medicine, National Cheng Kung University College of Medicine, 1 University Road, Tainan, Taiwan 70101, ROC. Tel: +88 66 235 3535 ext. 5592; Fax: +88 66 209 5845; E-mail: changns@mail.ncku.edu.tw
or F-J Lai, Department of Dermatology, Chi-Mei Medical Center, Tainan, Taiwan, ROC. Tel: +88 66 281 2811; Fax: +88 66 270 3706; E-mail: laifj@mail.ntin.edu.tw; or C-I Sze, Department of Anatomy and Cell Biology, National Cheng Kung University College of Medicine, 1 University Road, Tainan, Taiwan 70101, ROC. Tel: +88 66 235 3535 ext. 5329; Fax: +88 66 209 3007; E-mail: szec@mail.ncku.edu.tw
Keywords: TIAF1; p53; WWOX; WOX1; TGF-β; Smad4
Abbreviations: TGF-β, transforming growth factor β; TIAF1, TGF-β1-induced antiapoptotic factor; Aβ, amyloid β; WWOX/WOX1, WW domain-containing oxidoreductase; Smad4, mothers against DPP homolog 4; TNF, tumor necrosis factor; FRET, Förster resonance energy transfer; IHC, immunohistochemistry
Received 15.8.11; revised 10.2.12; accepted 14.2.12; Edited by A Stephanou

Treg and TH2 cells is unknown. TIAF1 is also associated with Hirschsprung's disease, a congenital complex disorder of intestinal innervation.[10]

TIAF1 physically interacts with Smad4, and blocks SMAD-dependent promoter activation when overexpressed.[11] Knockdown of TIAF1 by siRNA induces spontaneous accumulation of Smad proteins in the nucleus and activation of the promoter governed by the SMAD complex.[11] Notably, TGF-β1 and environmental stress (e.g. alterations in pericellular environment) cause TIAF1 self-aggregation in a type II TGF-β receptor (TβRII)-independent manner in cells. Hippocampal TIAF1 aggregation is shown at ages 40–70, which occurs before the generation of amyloid β (Aβ) plaques in Alzheimer's disease at 75–90-years.[11] Here, we examined TIAF1 expression and aggregate formation in cancer cells and tissues, and determined the functional relationship between TIAF1 and tumor suppressors WW domain-containing oxidoreductase (designated WWOX, FOR or WOX1)[12–14] and Smad4. TIAF1 control of SMAD-regulated promoter activation was examined.

Results

TIAF1 expression is upregulated in non-metastatic prostate cancer but is downregulated in breast cancer. A synthetic TIAF1 peptide R48-2, which was originally used for the antibody production,[5,11] blocked the immunoreactivity in antibody staining, as determined in human melanoma (Supplementary Figure S1a), neurofibromatosis NF1 tumor (Supplementary Figure S1b), meningioma (Supplementary Figure S1c) and breast cancer (Figure 1a and Supplementary Figures S2g–i) and other tissue sections. The R48-2 peptide also blocked the immunoreactivity of a commercial antibody TIAF1(Abcam, Cambridge, MA, USA) (Supplementary Figure S1a). We generated another TIAF1(R48-1) antibody using a different peptide sequence. The TIAF1(R48-2) peptide failed to inhibit the immunoreactivity of TIAF1(R48-1) antibody (Supplementary Figure S1c).

TIAF1 expression is shown in normal human mammary gland cells, as determined by immunohistochemistry (IHC) (Figure 1a and Supplementary Figure S2). In breast adenocarcinoma, the levels of TIAF1 are significantly reduced (Figure 1a and Supplementary Figure S2). In negative controls, the R48-2 peptide blocked the immunoreactivity of TIAF1 antibody (Figure 1a).

In prostate tissue microarray slides, TIAF1 levels are significantly increased in prostate cancer, compared with normal controls, as determined using both TIAF1(R48-2) and the commercial antibodies for fluorescence microscopy (Figure 1b; 75 samples for control and cancer groups and damaged samples excluded). Both antibodies recognized essentially the same TIAF1 antigen, as both images appear to colocalize (Supplementary Figure S1a). Similar results were observed using the TIAF1(R48-2) antibody in IHC (data not shown). We further confirmed these findings by using normal prostate and prostate cancer sections in immunofluorescence microscopy and IHC (Figure 1c, Supplementary Figures S3a and S4). Compared with age-matched normal controls, there were significant increases (50–120%) in the expression of TIAF1 in prostate cancer tissues (Supplementary Figures S3a and S4). In negative controls, R48-2 peptide blocked the immunoreactivity (Supplementary Figure S4).

TIAF1 aggregates in cancer cells. TIAF1 physically interacts with Smad4, and knockdown of TIAF1 expression induces spontaneous accumulation of Smad proteins in the nuclei.[11] By immunofluorescence microscopy, TIAF1 co-localized with Smad4 in the cytosol and prostatic concretions in the lumens of glandular ducts (Supplementary Figures S3b and S3c). Upregulation of TIAF1 and Smad4 is shown in the prostate cancer tissues (Figure 1c, Supplementary Figures S3 and S4). Both TIAF1 and Smad4 proteins are colocalized and appear as aggregates (Supplementary Figures S3b and S3c). Notably, expression of both TIAF1 and Smad4 are significantly downregulated in metastatic prostate cancer cells (Figure 1c and Supplementary Figure S5). Similarly, expression of TIAF1 and Smad4 proteins is significantly increased ($P<0.05$) in colon cancer cells, as compared with controls (Supplementary Figure S6). IHC staining of prostate with the TIAF1(R48-2) antibody showed a poorly differentiated tumor growing in a diffused fashion (Figure 1d). The tumor infiltrates the prostate as cell clusters, without glandular formation and containing TIAF1 protein aggregates (Figure 1d).

Next, hairless mice were exposed to UVB irradiation to generate skin squamous cell carcinoma (SCC).[15] TIAF1 is overexpressed in the sebaceous gland of the normal skin (Figure 1e). UVB rapidly increased the expression of TIAF1 in the epidermis in 12 h, followed by reduction. However, in the dermal area, TIAF1 levels were increased from 24 h to 1 month after UVB exposure. The developed SCC tumors had reduced expression of TIAF1 (Figure 1e).

TIAF1 aggregation in the metastatic cancer cells in the brain. TIAF1 aggregates are present in the hippocampi of both non-demented humans and patients with Alzheimer's disease.[11] Co-expression of TIAF1 and Aβ aggregates was found in the metastatic cancer in the brain (Figures 2a and b). Conceivably, when metastatic small-cell lung cancer cells relocated to the brain, TIAF1 aggregates were deposited in the interface between cancer and brain cells or within the tumors (Figures 2a and b, Supplementary Figures S7 and S8). Fluoro-Jade C stain[11] demonstrated the presence of degenerating neurons (Figures 2a and b, Supplementary Figures S7 and S8). In negative controls, R48-2 peptide blocked the immunostain (Figures 2a and b, Supplementary Figures S7 and S8). Similarly, co-expression of the aggregates for TIAF1 and Aβ was shown for the metastatic lung cancer, nasopharyngeal carcinoma (NPC) and colon cancer in the brain (Figure 2b, Supplementary Figures S7 and S8). Despite the presence of Aβ, no apparent apoptosis was observed in the cancer cells.

Compared with TIAF1, WOX1 expression is relatively low in neurofibromatosis NF1 (Figures 2c and d). TIAF1 is overexpressed in the peritumor area (Figure 2d). Alteration of environmental cues induces TIAF1 expression and aggregation.[11] Presence of fibrous aggregation of TIAF1 is shown in the peritumor coat of NF1 (Figure 2e), prostate cancer (Supplementary Figure S9), many solid tumors and hippocampi of patients with Alzheimer's disease (data not

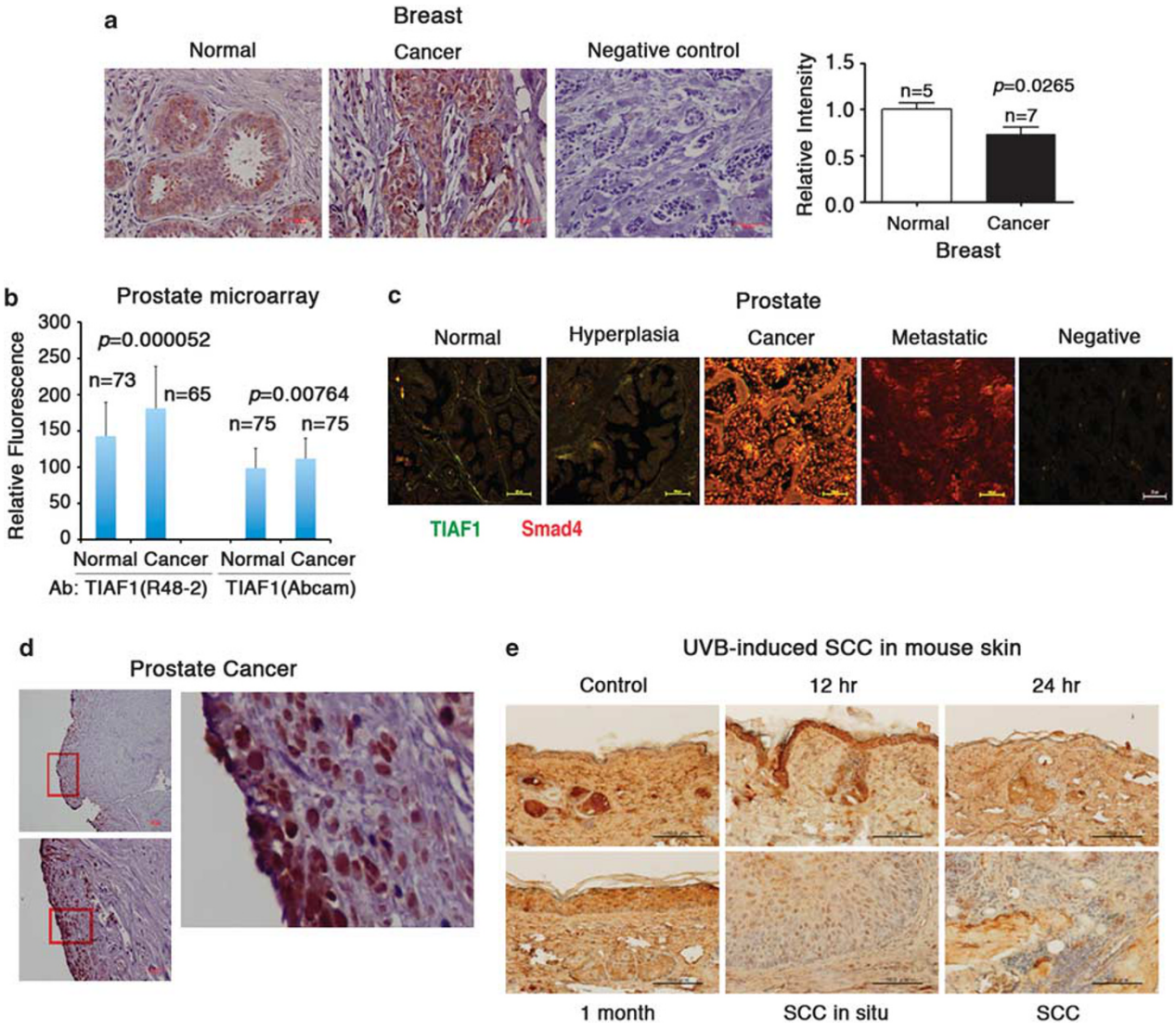

Figure 1 TIAF1 expression in breast, prostate and skin cancers. (**a**) IHC staining of normal and breast cancer tissue sections revealed a significant reduction of TIAF1 in the cancer tissues, using TIAF1(R48-2) antibody (Student's *t*-test). In negative control, R48-2 peptide blocked the immunoreactivity of the antibody. Also, see additional data in Supplementary Figure S2. (**b**) TIAF1 protein expression is significantly increased in prostate cancer, compared with normal controls, as determined using both the TIAF1 (R48-2) antibody (left panel) and a commercial TIAF1 antibody (right panel) for immunofluorescence microscopy in prostate tissue microarray slides from NCI (Student's *t*-test).[11,17,35,39] Also, see data in Supplementary Figures S3, S4 and S5. (**c**) By immunofluorescence microscopy, significant increases (50–120%) in the TIAF1 protein expression were shown in prostate cancer tissues (three cases), as compared with samples from age-matched normal controls, prostatic hyperplasia and metastatic prostate cancer. In negative controls (Negative), non-immune serum was used for staining. Scale bar, 100 μm; $\times$ 100 magnification. Merged images of TIAF1 (green) and Smad4 (red) are shown. Also, see detailed pictures in the Supplementary Figure S5. (**d**) A poorly differentiated tumor grew in the prostate as cell clusters with no glandular formation but contained TIAF1 protein aggregates. Graphs are sequentially enlarged from each red box (from top left, bottom left to right). (**e**) UVB irradiation induced formation of SCC in hairless mice. TIAF1 protein expression is abundant in the sebaceous gland of the normal skin. The developed SCC tumors have low levels of TIAF1. Scale bar = 50 μm

shown). Again, R48-2 peptide blocked the immunoreactivity (Figure 2f).

When metastatic 13-06-MG glioma cells were subcutaneously inoculated in both flanks of nude mice, the cells were metastatic to the lung. Presence of high levels of TIAF1 expression is shown in the growing tumor, compared with the normal lungs of nude mice (Figure 2g).

Extracellular matrix (ECM) proteins induce the expression and aggregation of TIAF1 and Aβ, and ectopic WOX1 upregulates TIAF1 expression. To simulate the encounter of metastatic cancer cells with brain cells, neuroblastoma SK-N-SH cells were cultured on the ECM of prostate DU145 cells for 48 h.[11,16] SK-N-SH cells were shown to have overexpressed aggregates of TIAF1 and Aβ, as determined by fluorescent immunostaining (Figures 3a and b). However, when the endogenous TIAF1 level was low, Aβ expression was also low (Figure 3b). In negative controls, cells were seeded onto serum protein-coated matrix where no TIAF1 and Aβ production was observed (data not shown).

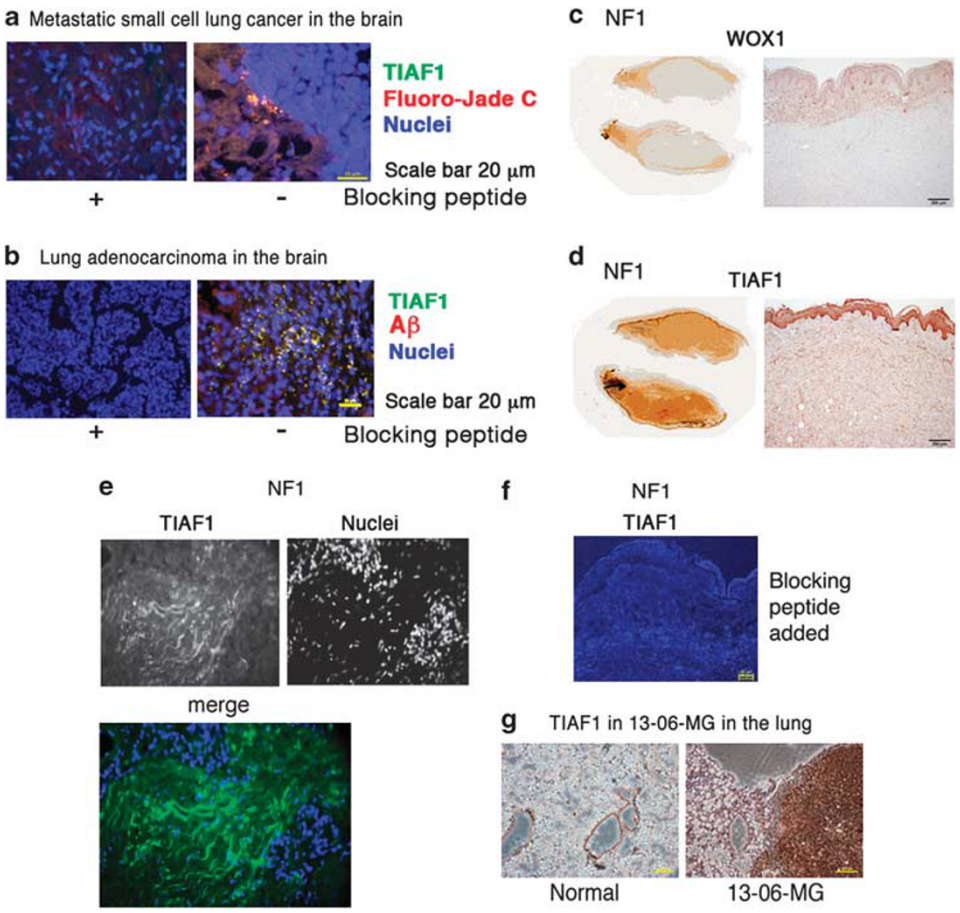

Figure 2 TIAF1 aggregation in the interface between metastatic cancer cells and the brain tissues. (**a**) Presence of aggregated TIAF1 in the dead neurons located in the interface between the brain tissue and the metastatic small-cell lung cancer. Degenerating neurons were stained with Fluoro-Jade C (red). Nuclei were stained with DAPI. Scale bar, 20 μm; $\times$ 400 magnification. A merged image is of TIAF1 (green), Fluoro-Jade C (red) and DAPI (blue). The blocking R48-2 peptide was used in negative controls. Also, see Supplementary Figures S7 and S8. (**b**) TIAF1/Aβ aggregates are shown in a metastatic lung adenocarcinoma in the brain. Scale bar, 20 mm; $\times$ 400 magnification. A merged image is of TIAF1 (green), Aβ (red) and DAPI (blue). The blocking R48-2 peptide was used in negative controls. (**c** and **d**) In IHC staining, expression of WOX1 and TIAF1 is shown in neurofibromatosis NF1. TIAF1 is overexpressed in the peritumor area, but is less expressed in the tumor itself. Scale bar, 100 μm. (**e**) Fibrous protein aggregates are shown in the peritumor coats of neurofibromas. TIAF1 is present in the fibrous aggregates ($\times$ 400 magnification). (**f**) R48-2 peptide was used to block the immunoreactivity in the negative control staining. (**g**) Metastatic 13-06-MG glioma cells were subcutaneously inoculated and shown to metastasize to the lung of a nude mouse. The growing tumor in the lung showed a high level expression of TIAF1 as compared with the normal lung of a nude mouse. Scale bar, 200 μm; $\times$ 400 magnification (IHC). A representative data set is shown from three repeats

Also, petri dishes were coated with various amounts of matrix proteins from DU145, followed by seeding with SK-N-SH cells. Two days later, SK-N-SH cells were harvested and shown to have increased levels of polymerized Aβ (Figure 3c). The smallest unit of Aβ is $\sim$4 kDa. Similar results were observed by culturing SK-N-SH cells on the matrix of many other types of cancer cells such as breast MCF7 and lung NCI-H1299 cells (data not shown).

We simulated the potential effects of brain metastatic cancer cells on neural cells by co-culturing. SK-N-SH cells were co-cultured with COS7 fibroblasts, followed by determining the expression of TIAF1. SK-N-SH cells were transiently overexpressed with enhanced cyan fluorescence protein (ECFP), and COS7 cells with EYFP. When both cells were co-cultured for 24 h, TIAF1 was not induced (Figures 3d and e). However, transiently overexpressed EYFP-WOX1 dramatically induced TIAF1 expression in COS7 cells (Figures 3d and e).

Aggregating TIAF1 induces spontaneous activation of SMAD-responsive promoter in p53-deficient NCI-H1299 cells. TIAF1 physically interacts with Smad4 and suppresses the SMAD-driven promoter activation.[11] When COS7 cells were transiently overexpressed with Smad4, in the presence of a SMAD promoter plasmid (containing green fluorescence protein (GFP) as reporter), the promoter became activated (Figure 4a). Transiently overexpressed TIAF1 blocked Smad4-induced promoter activation (Figure 4a). When p53-deficient NCI-H1299 cells were transfected with TIAF1 or WOX1, in the presence of the SMAD promoter plasmid, spontaneous activation of the promoter occurred (Figure 4b). TIAF1 was tagged with

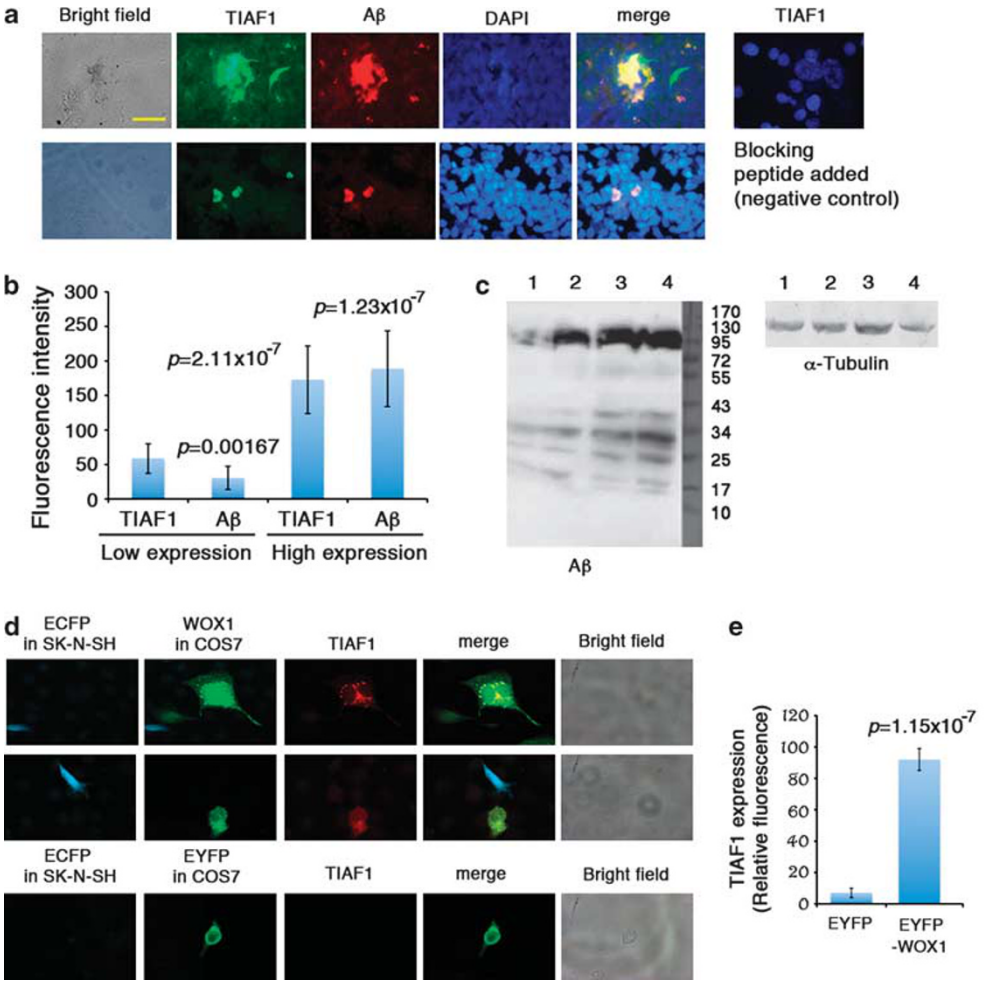

Figure 3 ECM proteins induce the expression and aggregation of TIAF1 and Aβ, and ectopic WOX1 upregulates TIAF1 expression. (**a**) Neuroblastoma SK-N-SH cells were cultured on the ECM of prostate DU145 cancer cells. Extracellular protein matrix from DU145 cells was prepared as described.[11,16] Note that TIAF1 and Aβ protein aggregates are colocalized or exist alone. In negative controls, R48-2 blocking peptide was used in the immunostaining (merge of DAPI and TIAF1 images). Two representative data are shown from three experiments ($\times$ 400 magnification; 50 cells examined per experiment). (**b**) Data are tabulated for endogenous TIAF1 expression at low and high levels, relative to the expression of Aβ (mean $\pm$ S.D.; Student's *t*-test; $n = 3$; all data *versus* low expression TIAF1 controls).[11,17,35,39] In negative controls, cells were seeded onto serum proteins-coated matrix, which did not induce TIAF1 and Aβ production. Fluorescence intensity was <25. (**c**) Petri dishes were coated with various amounts of matrix proteins from DU145, followed by seeding with SK-N-SH cells. Two days later, Western blotting for Aβ expression was performed. Aβ is polymerized to various sizes. The monomeric Aβ is $\sim$4 kDa. Coated proteins: lane 1, 0 μg; lane 2, 1 μg; lane 3, 2 μg; and lane 4, 4 μg. α-tubulin is regarded as protein-loading control. (**d** and **e**) SK-N-SH cells were expressed with ECFP, and COS7 cells with EYFP or EYFP-WOX1. Co-culture of ECFP-SK-N-SH and EYFP-COS7 cells did not result in induction of TIAF1 expression. However, ECFP-WOX1 alone was sufficient to induce TIAF1 expression in COS7 cells (mean $\pm$ S.D.; Student's *t*-test; n = 3; 50 cells examined per experiment)[11,17,35,39]

Discosoma species red fluorescent protein (DsRed). However, when TIAF1 was tagged with monomeric DsRed, no spontaneous activation of the SMAD-governed promoter was observed (Figure 4b). TIAF1, tagged with DsRed, EGFP, ECFP or EYFP, tended to aggregate, whereas monomeric DsRed-TIAF1 (TIAF1dm) remained mainly as monomer.

TIAF1 self-association induces expression of Smad4 and WOX1. In agreement with our previous observations,[11] ectopic expression of TIAF1 tagged with ECFP or EYFP (ECFP-TIAF1 or EYFP-TIAF1) in breast MCF7 cells resulted in an increased self-binding, as determined by FRET (Förster resonance energy transfer) analysis (Figure 5a).[11,17] The TIAF1 self-binding led to an increased expression of Smad4, and both Smad4 and TIAF1 colocalized in the cytoplasm and cellular protrusion (Supplementary Figure S10). TGF-β1 marginally reduced the effects (Figure 5a).

By non-reducing SDS-PAGE and western blotting, transiently overexpressed EGFP-TIAF1 induced the expression of Smad4 and WOX1 in MCF7 (Figure 5b) and other types of cancer cells (data not shown). TIAF1 self-polymerized, as the molecular sizes are $>$95 kDa (TIAF1 monomer, 12 kDa; EGFP-TIAF1, 44 kDa). Prima-1, an activator of p53,[18] further increased TIAF1 polymerization by more than 200 kDa (Figure 5b). The induced Smad4 exhibited as a monomer (Figure 5b). Under the influence of ectopic TIAF1, WOX1 polymerized from a monomer $\geq$46 kDa (Figure 5b). In parallel, ectopic EGFP-TIAF1 formed cytoplasmic punctate aggregates, with concurrent expression of WOX1 (Figure 5c).

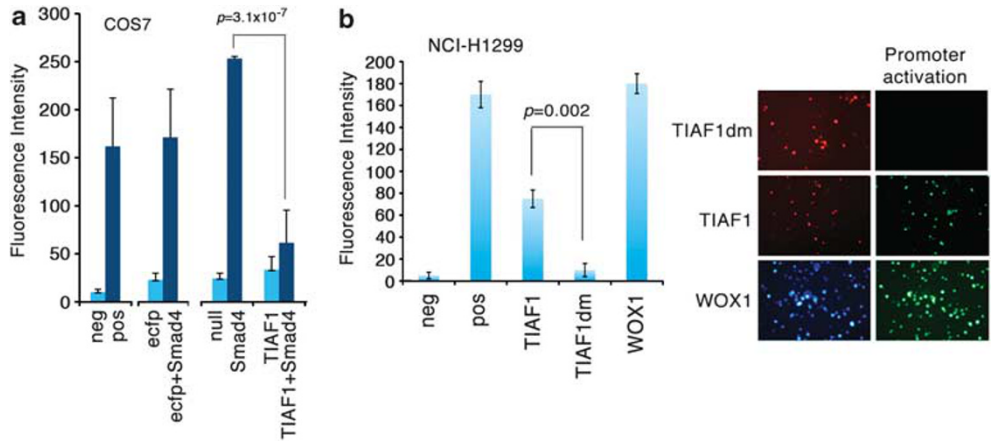

Figure 4 TIAF1 self-aggregation is essential for causing spontaneous activation of a SMAD-responsive promoter in p53-deficient cells. (**a**) COS7 cells were transfected by liposome with plasmids for expressing ECFP, ECFP-Smad4, ECFP-TIAF1 and/or a GFP-reporting plasmid with a SMAD-responsive element.[17,35] In controls, cells were transfected with a negative or a positive plasmid. After 24 h, the cells were imaged by fluorescence microscopy. The extent of promoter activation was measured (mean ± S.D.; Student's *t*-test; $n=3$).[17,35] Smad4 induced the promoter activation, whereas TIAF1 suppressed the effect. Similar results were observed by tagging Smad4 or TIAF1 with DsRed (data not shown). neg, negative control; pos, positive control; null, electroporation with medium only. (**b**) p53-deficient NCI-H1299 cells were transfected with DsRed-TIAF1, TIAF1dm or ECFP-WOX1, in the presence of the SMAD promoter plasmid. DsRed-TIAF1 induced spontaneous activation of the SMAD-governed promoter, whereas the monomeric DsRed had no effect. A representative set of promoter activation is shown (right panel). Both negative and positive controls were included in the experiments (mean ± S.D.; Student's *t*-test; $n=3$)

Both EGFP and dominant-negative EGFP-TIAF1[11] failed to induce WOX1 expression (Figure 5c). When TIAF1 was tagged with monomeric DsRed, no aggregate formation was observed (data not shown).

Endogenous TIAF1 aggregate formation requires culturing two distinct cell types on non-self ECM. By co-culturing both COS7 fibroblasts and neuroblastoma SK-N-SH cells on the ECM of prostate DU145 cells for 48 h, endogenous TIAF1 became punctate aggregates in the cytoplasm of both cells, as determined by using specific TIAF1(R48-2) antibody (top two rows; Figure 5d). WOX1 expression was also increased (Figure 5d). No TIAF1 aggregate formation was observed by culturing COS7 cells alone on the ECM (Figure 5d). Again, the R48-2 blocking peptide abolished the immunofluorescence (Figure 5d). The observations suggest that when two distinct types of cells encounter each other, endogenous TIAF1 aggregation may occur.

TIAF1-/Smad4-binding induces generation of amyloid precursor protein (APP) and Aβ. p53-deficient NCI-H1299 cells were transiently overexpressed with ECFP-Smad4 and EYFP-TIAF1. The cells were treated with TGF-β1 for 24 h, which resulted in an increased generation of APP and Aβ (Figure 5e). By FRET analysis, TGF-β1 increased the binding of Smad4 and TIAF1 (Figure 5e). Similar results were also obtained using p53-positive MCF7, COS7 and L929 cells (data not shown).

TIAF1 is required for WOX1-, p53- and dominant-negative JNK1 (dnJNK1)-mediated apoptosis. We examined whether TIAF1 participates in WOX1- and p53-mediated apoptosis. TGF-β-sensitive mink lung epithelial Mv1Lu cells were transfected with expression constructs of WOX1 and/or siRNA-targeting TIAF1 (TIAF1si)[5,7] by electroporation, followed by culturing for 48 h. In controls, a 'scrambled RNA' plasmid was used in transfection. When endogenous TIAF1 was knocked down by siRNA, WOX1-induced growth inhibition of Mv1Lu cells was blocked (Figure 6a).

Similarly, L929 cells were transfected with the expression plasmids of WOX1 and/or TIAF1si by electroporation, and were then grown in soft agarose for 3 weeks. Presence of live colonies was measured using MTS proliferation assay.[7] WOX1 significantly inhibited the anchorage-independent growth of L929 cells ($P<0.001$; $n=3$; Student's *t*-test), when compared with control cells transfected with the 'scrambled RNA' plasmid (Figure 6b). However, WOX1 did not inhibit the growth of TIAF1si-expressing cells ($P>0.05$; $n=3$; Student's *t*-test), suggesting that WOX1-induced growth suppression is TIAF1-dependent.

WOX1 and TIAF1 worked synergistically to induce cell death. Transient expression of low levels of WOX1 or TIAF1 did not cause L929 cell death (<10%) (Figure 6c). When in combination, both WOX1 and TIAF1 significantly caused cell death (~40%) (Figure 6c). Dominant-negative WOX1 (dnWOX1) alone did not induce cell death, in the absence or presence of TIAF1 (Figure 6c). dnWOX1 is known to block the apoptotic functions of p53 and WOX1.[12–14,17] Alteration of Tyr33 and Tyr61 in WOX1 abolishes its apoptotic function, and no enhancement of apoptosis occurred in the presence of TIAF1 (Figure 6c). Tyr61 is a conserved phosphorylation site and its phosphorylation status has been confirmed by specific antibody (Chang *et al*., unpublished).

We determined whether TIAF1 or WOX1 knockdown causes resistance to p53-dependent apoptosis. L929 cells, which were stably transfected with a scramble, TIAF1si or WOX1si construct, were electroporated with an empty vector, a p53 or a dnJNK1 expression plasmid. In agreement with our previous studies,[12,19,20] both transiently overexpressed p53

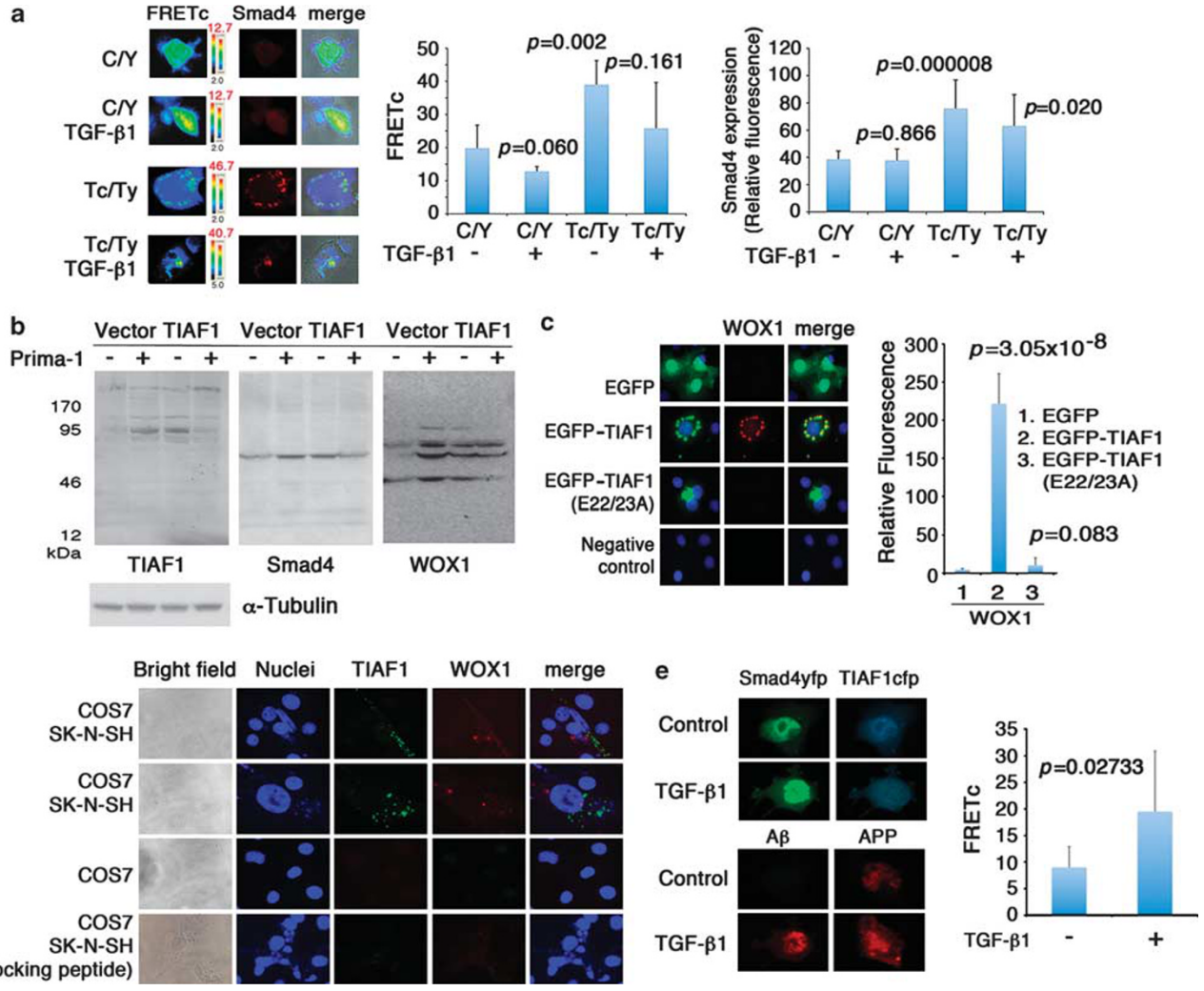

Figure 5 TIAF1 self-association induces expression of Smad4 and WOX1. (**a**) MCF7 cells were transiently transfected with ECFP and EYFP (C/Y) or ECFP-TIAF1 and EYFP-TIAF1 (Tc/Ty) by liposome. The cells were treated with or without TGF-β1 (5 ng/ml) for 24 h. TIAF1 self-binding was analyzed by FRET microscopy.[11,17,35] FRETc shows the extent of protein/protein binding.[11,17,35] TIAF1 self-binding led to Smad4 expression, as determined by immunofluorescence staining. Statistical analysis: all tests *versus* C/Y controls; Student's *t*-test ($n = 6$). The induced Smad4 colocalized with TIAF1 in the cytoplasm and the spiny protrusion ($\times$ 400 magnification; Supplementary Figure S10). (**b**) Transiently overexpressed EGFP-TIAF1 upregulates the expression of Smad4 and WOX1 in MCF7 (non-reducing SDS-PAGE) and other types of cancer cells (data not shown). Exposure of cells to Prima-1 (10 μM) for 1 h to activate p53 resulted in increased polymerization of TIAF1 and WOX1, but not Smad4. (**c**) COS7 cells were transiently overexpressed with EGFP-TIAF1 or EGFP. Significantly increased expression of WOX1 is shown, where these proteins colocalize with TIAF1 aggregates, as determined using specific antibodies ($n = 10$; mean $\pm$ S.D.; experiments *versus* EGFP controls, Student's *t*-test). Dominant-negative TIAF1 (E22/23A) and EGFP failed to induce the indicated protein expression. (**d**) To stimulate endogenous TIAF1 aggregate formation, COS7 and/or SK-N-SH cells were co-cultured on the ECM of prostate DU145 cells for48 h. Aggregate formation of endogenous TIAF1, along with WOX1 expression, is shown in the cytoplasm of both cells (top two rows). No TIAF1 aggregate formation was observed by culturing COS7 cells alone on the ECM (third row from the top). R48-2 blocking peptide abolished the immunofluorescence (bottom row). (**e**) NCI-H1299 cells were transiently overexpressed with ECFP-Smad4 and EYFP-TIAF1, followed by treating with TGF-β1 (5 ng/ml) for 24 h. Increased binding of Smad4 and TIAF1 positively correlates with upregulation of APP and Aβ

and dnJNK1 caused apoptosis of control cells (Figure 6d). TIAF1 or WOX1 knockdown cells resisted death caused by the transiently overexpressed p53 and dnJNK1 (Figure 6d). In contrast, when TIAF1 was knocked down in Mv1Lu cells, apoptosis caused by transiently overexpressed Smad4 was increased (subG1 phase; Figure 6e).

TIAF1, WOX1 and p53 synergistically induce apoptosis and block anchorage-independent growth and cell migration. We investigated whether TIAF1, WOX1 and p53 act synergistically in causing apoptosis. L929 fibroblasts were grown on cover slips overnight, and co-transfected with non-apoptosis-inducing amounts of p53, WOX1 and/or TIAF1 plasmid constructs by the liposome-based Gene Fector (Venn Nova, Pompano Beach, FL, USA). The cells were then grown for 48 h. When in combination, TIAF1, p53 and WOX1 dramatically induced apoptosis in a synergistic manner ($\sim$75%) (Figure 7a). The combination of TIAF1/p53, p53/WOX1 or TIAF1/WOX1 had a much less effect in inducing apoptosis (0–25%) (Figure 7a). Similar results were

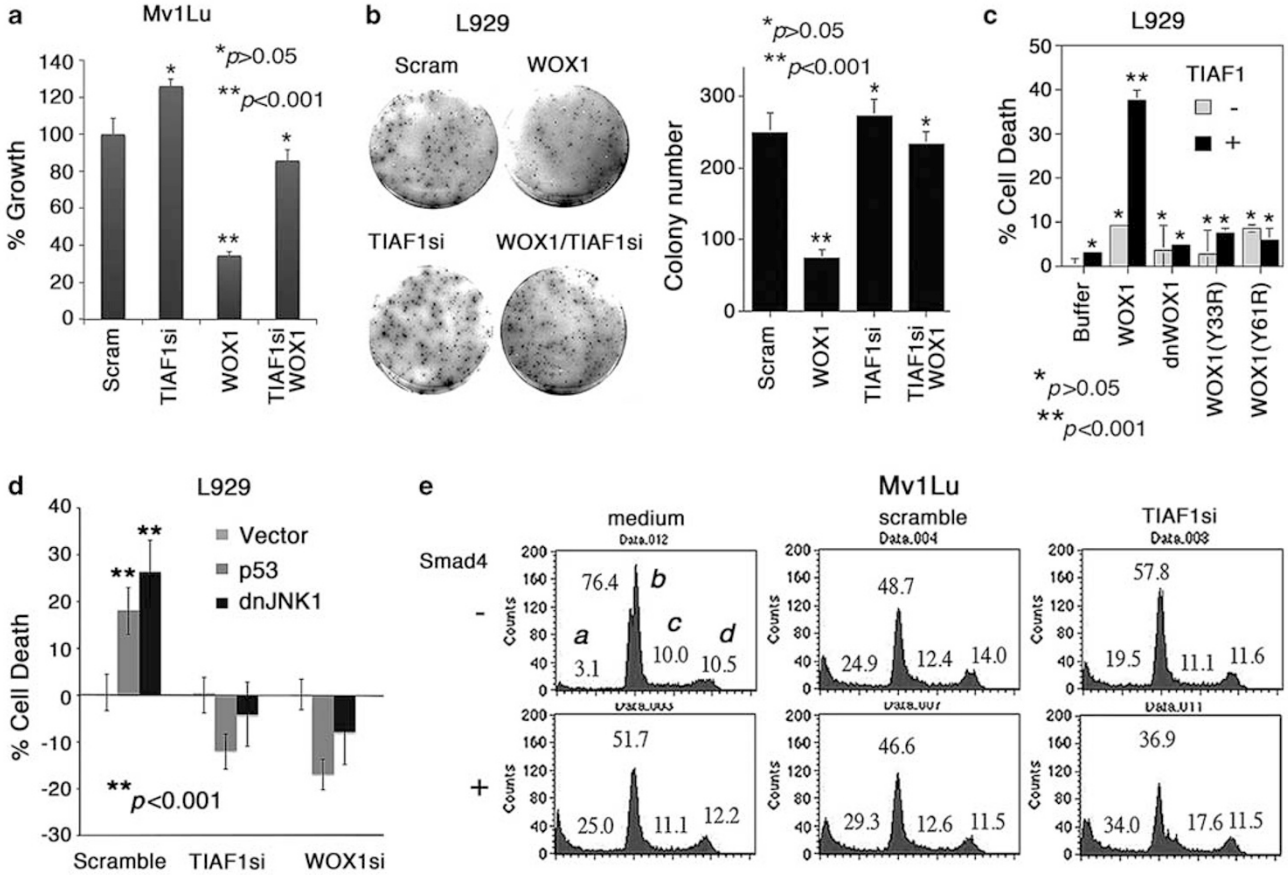

Figure 6 TIAF1 is essential for apoptosis mediated by WOX1, p53 and dominant-negative JNK1. (**a**) Mv1Lu cells were transfected with expression plasmid constructs of WOX1 and/or TIAF1si by electroporation, followed by culturing for 48 h. The extent of cell growth was measured by MTS proliferation assay. TIAF1 knockdown cells resisted WOX1-induced growth inhibition ($n=8$; mean ± S.D.; Student's *t*-test: experiments *versus* scramble controls). Scram = 'scrambled RNA' control plasmid. (**b**) L929 cells were transfected with WOX1 and/or TIAF1si plasmids, and then grown in soft agarose for 3 weeks to allow colony formation (measured by MTS proliferation assay) ($n=3$; Student's *t*-test; experiments *versus* scramble controls). (**c**) When L929 cells were transfected with WOX1 and TIAF1 plasmids (1.25 μg per 10^6 cells), both expressed proteins synergistically caused cell death (~40%, n = 8). Dominant-negative WOX1 (dnWOX1)[17] and phospho-WOX1 mutants (Y33R and Y61R)[17] failed to induce cell death, in the absence or presence of TIAF1 ($n=8$; Student's *t*-test: experiments *versus* scramble controls). (**d**) L929 stable transfectants, expressing a scramble, TIAF1si or WOX1si construct, were established. Transient overexpression of these cells with an empty vector, p53 or dnJNK1 construct was carried out, and the extent of cell death was measured in 48 h ($n=8$; Student's *t*-test; experiments *versus* scramble controls). When TIAF1 and WOX1 were knocked down, ectopic p53 and dnJNK1-induced cell death was blocked. (**e**) In contrast, when TIAF1 was knocked down, Smad4-induced apoptosis of Mv1Lu cells was enhanced (see subG1 phase; a representative data from two experiments). *a*, SubG1 phase; *b*, G0/G1 phase; *c*, S phase; *d*, G2/M phase

also observed in COS7, NCI-H1299 and other cells (data not shown).

When L929 cells were co-transfected with the above constructs, followed by performing anchorage-independent growth, TIAF1, p53 and WOX1 together dramatically suppressed colony formation by >95% (Figure 7b). Each protein alone blocked colony formation by ~50%, and that two proteins together increased the suppression up to 65–90% (Figure 7b). We have previously shown that p53 and TIAF1 together effectively block the anchorage-independent growth of L929 cells.[7]

In parallel experiments, ectopic expression of p53, WOX1 and TIAF1 significantly blocked the migration of L929 and breast MDA-MB231 cells during the observation for 16 h (Figure 7c and Supplementary Figure11a). Non-apoptosis-inducing levels of expression plasmids for p53, WOX1 and TIAF1 were used in introducing into cells. The effect was observed by testing each protein alone or in various combinations. Interestingly, under similar conditions, ectopic p53, WOX1 and TIAF1 in combination were less effective in blocking the migration of breast MCF7 than those of p53 and WOX1 alone (Supplementary Figure S11b).

Of particular note is that when normal cells such as fibroblasts and cardiomyocytes were expressed with p53, WOX1 and TIAF1, these cells became highly sensitive to death induced by cytokines TNF-α and TGF-β1 in 4 h (data not shown). Again, the observations suggest that p53, WOX1 and TIAF1 can act in concert to drive the cell death event.

Discussion

In summary, we have determined that (1) TIAF1, along with Smad4 and Aβ, participates in the formation of peritumor capsules, which is crucial for solid tumor growth and protection; (2) under the stimulation of non-self ECM, endogenous TIAF1 is upregulated and undergoes

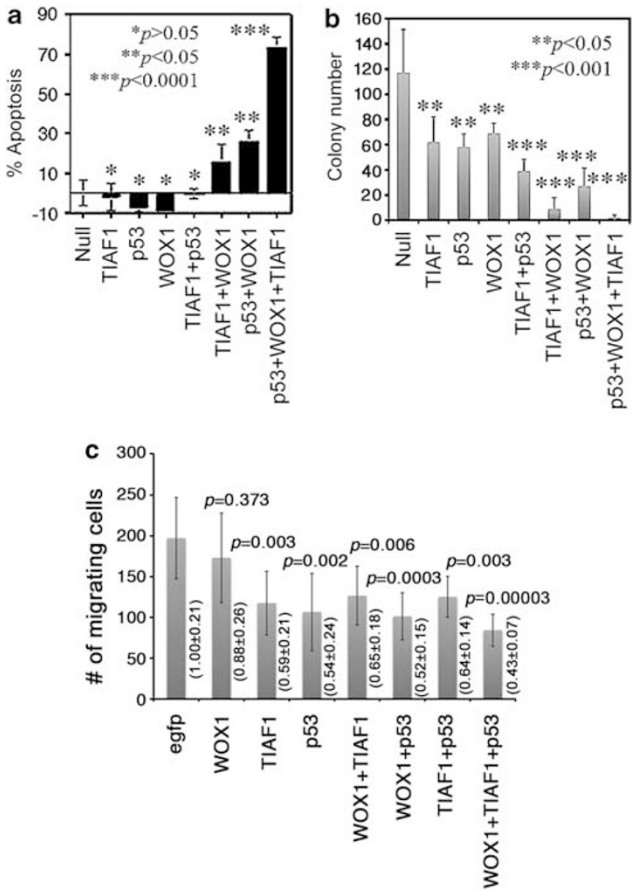

Figure 7 TIAF1, WOX1 and p53 synergistically induce apoptosis, block cell migration and inhibit anchorage-independent growth. (**a**) L929 cells were co-transfected with non-apoptosis-inducing amounts of wild-type p53, WOX1 and/or TIAF1 plasmid constructs (2.5 μg) by the liposome-based GeneFector. The extent of cell death was measured by nuclear morphology. Nuclei were stained with DAPI (mean ± S.D.; $n=8$; Student's *t*-test). (**b**) L929 cells were transfected with the above constructs by electroporation, and then subjected to performing anchorage-independent growth assay. After 3 weeks, the live cell colonies were measured by staining with the MTS proliferation assay (mean ± S.D.; $n=8$; Student's *t*-test). (**c**) Under similar conditions, L929 cells were transfected with non-apoptosis-inducing amounts of wild-type p53, WOX1 and/or TIAF1 plasmid constructs. The transiently overexpressed p53, WOX1 and TIAF1, alone or in combinations, significantly blocked the migration of L929 cells (mean ± S.D.; $n=3$; Student's *t*-test). *P* value is shown on the top of each bar. The number in each bracket is 'fold increase' in cell migration

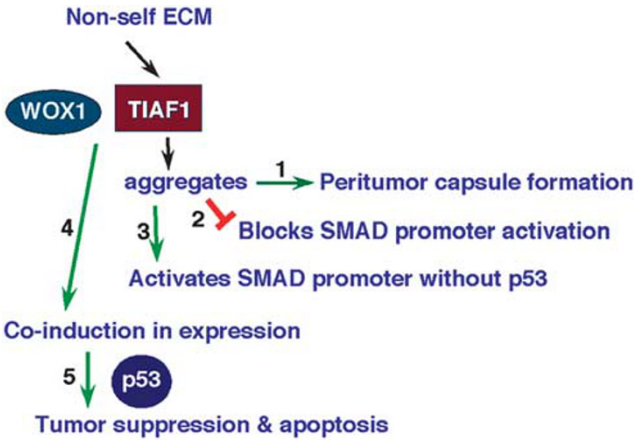

Figure 8 TIAF1 aggregation and associated events. (1) Under environmental alterations (e.g., non-self ECM), endogenous TIAF1 is prone to aggregation, which is critical for supporting peritumor capsule formation; (2) During self-aggregation, TIAF1 binds Smad4 and blocks SMAD promoter activation; (3) Intriguingly, under p53-deficient conditions, aggregating TIAF1 supports the activation of the SMAD-governed promoter; (4) Overexperssed TIAF1 induces WOX1 expression, and vice versa; (5) TIAF1, p53 and WOX1 act synergistically in causing growth suppression and cell death

aggregation, which binds Smad4 and blocks SMAD promoter activation;[11] (3) however, in the absence of p53, the aggregating TIAF1 activates the SMAD-governed promoter; (4) increased levels of TIAF1 induces WOX1 expression, and vice versa; (5) TIAF1 is essential in the p53- and WOX1-mediated cell death, and these proteins act synergistically in inducing cell death (Figure 8).

Alteration of TIAF1 levels appears to affect cancer progression. We showed that UVB-induced SCC formation in rats is associated with an initial upregulation of TIAF1, followed by reduction in the cancer. This expression profile positively correlates the expression of WOX1 protein during SCC development.[15] Also, TIAF1 is accumulated in developing metastatic tumor cells when growing in a new organ site. Once the metastatic solid tumors become established, TIAF1 is significantly downregulated. The observation suggests that TIAF1 is central to cancer progression. TIAF1 may exhibit as fibrous aggregates, together with Smad4, Aβ and other proteins, in the stromal tissues of tumors and peritumor capsules. Also, both TIAF1 and Smad4 are co-present in the normal prostatic concretions in the lumens of prostatic glandular ducts, and they are intracellular proteins. How these proteins become secreted remains to be established. Whether the extracellular TIAF1 and Smad4 are functionally inactive is unknown.

A developing tumor circumvents pericellular and environmental challenges. It is not surprising to see dramatic upregulation or downregulation of critical proteins, either intracellular or extracellular, in a single cancer cell during division and continuous expansion.[21,22] For example, during metastasis, cancer cells frequently have reduced expression of tumor suppressors probably because of gene mutation or epigenetic inactivation.[23,24] These cells may utilize strategies by significantly increasing the production of TGF-β, hyaluronan, hyaluronidases, metalloproteinases, gain-of-function isoforms of tumor suppressors and others to facilitate migration to target organs.[25-27] In contrast, at the benign stage, physical protection is built surrounding the peritumor area for allowing the growth and formation of a solid tumor.[28,29]

In our previous study, we have shown that TIAF1 aggregation in the hippocampus is essential for amyloid β deposition and formation of fibrils and plaques.[11] What leads to TIAF1 self-aggregation is largely unknown. We have determined that under the stress of cytokines or chemicals and/or alteration of pericellular matrix, TIAF1 becomes self-associated or aggregated.[11] In this study, we further demonstrated that upon co-culturing of COS7 and SK-N-SH cells on the ECM of

prostate DU145 cells, endogenous TIAF1 and WOX1 are upregulated and become aggregated. The observations support the scenario that an unfriendly environment induces endogenous TIAF1 aggregation. TGF-β rapidly induces TIAF1 self-aggregation, which leads to apoptosis in a caspase-dependent manner in certain cells.[11] Overexpressed TIAF1 affects Smad signaling and transcriptional activation. TIAF1 binds Smad4 *in vivo*, and blocks Smad-dependent promoter activation. Accordingly, when TIAF1 protein expression is knocked down by siRNA, spontaneous accumulation of Smad proteins in the nucleus occurs, along with activation of the SMAD-regulated promoter.[11] Interestingly, TGF-β1 induces TIAF1 self-aggregation in a TβRII-independent manner, and this may be related with binding of TGF-β1 to membrane hyaluronidase Hyal-2.[17] Indeed, TGF-β is able to signal via a Smad-independent manner for activation of NF-κB and JNK,[30] induction of lymphoid enhancer-binding factor (Lef-1) transcription factor,[31] and terminal skeletal muscle differentiation.[32]

TIAF1 is a likely gatekeeper in regulating cancer progression. TIAF1 is upregulated during the early stage of SCC formation. The developed SCC tumor has reduced TIAF1 expression. In prostate cancer, TIAF1 is most upregulated in the cancerous stage, but is downregulated during cancer metastasis. Interestingly, the expression profile of tumor suppressor WOX1 exhibits similarly to that of TIAF1 during cancer progression *in vivo*.[15,33,34] That is, both WOX1 and TIAF1 are significantly upregulated during the early phases of benign tumor formation. However, both proteins are downregulated when tumors possess metastatic potential. We determined that ectopic WOX1 induces the expression of TIAF1. WOX1 is known to enhance the transcriptional activation of SMAD and NF-κB promoters,[17,35] suggesting that TIAF1 expression is controlled by both promoters. TIAF1 in turn induces the expression of Smad4 and Aβ, depending upon the status of TIAF1 self-aggregation. TIAF1/Aβ aggregates are 'natural and protective fences' for both cancer and neural cells, but are likely to induce neurodegeneration during long-term exposure.

TIAF1 self-binding is essential for increasing the expression of Smad4 and WOX1. The underlying mechanism is unknown. Interestingly, the induced Smad4 colocalizes with TIAF1, and WOX1 appears to undergo self-association or binding with other proteins. Smad4 is able to interrupt the TIAF1 aggregation.[11] We have shown that when cells possess a greater amount of TIAF1 than Smad4, these cells survive upon challenge with TGF-β1. However, when cells express a greater amount of Smad4 than TIAF1, they were highly sensitive to TGF-β1-induced apoptosis.[11] In this study, we have confirmed the observations by TIAF1 knockdown and shown increases in Smad4-mediated apoptosis. Thus, a dynamic balance between Smad4 and TIAF1 is critical for cell survival.

We provided supporting evidence that TIAF1 is essential in the p53, WOX1 and dnJNK1-mediated cell death. And, these proteins can act synergistically in inducing cell death. How TIAF1 has such crucial effects is unknown. Conceivably, a direct interaction between TIAF1 and WOX1 occurs, which further connects the binding with p53. This scenario needs further study.

Materials and Methods

Cell lines, prostate cancer tissue microarrays, cancer tissue sections, IHC, antibodies and synthetic peptides. Cell lines used in the study were monkey kidney COS7 fibroblasts, murine L929 fibroblasts, mink lung Mv1Lu cells, human breast MCF7 and MDA-MB-231 cells, human lung NCI-H1299 cells, human neuroblastoma SK-N-SH cells and human prostate DU145 cells (American Type Culture Collections, Manassas, VA, USA). Purified human platelet-derived TGF-β1 and recombinant TGF-β1 were purchased from R&D Systems (Minneapolis, MN, USA) and PeproTech (Rocky Hill, NJ, USA), respectively. Prostate cancer tissue microarray slides (T-RP-2D), containing 75 samples each for control and cancer groups, respectively, were obtained from the Tissue Array Research Program, National Cancer Institute (Bethesda, MD, USA). In addition, human cancer tissue sections were obtained from the Department of Pathology, University of Colorado Health Sciences Center (by Dr. CI Sze, before 2005). IRB approval was waived. Informed consents were obtained from the family members of the deceased patients. Also, cancer tissue sections were obtained from the MacKay Memorial Hospital, Taipei, Taiwan (by Dr. MF Chiang) with IRB approval. De-parafinization, IHC and immunofluorescence staining were performed as described.[11,36] Presence of autofluorescence in each tissue section was examined by fluorescence microscopy. In most cases, we pre-blocked the autofluorescence of tissues by Sudan Black B (Sigma, St. Louis, MO, USA) before immunostaining.[37]

Specific homemade antibodies were against TIAF1(R48-2)[5,11] and WOX1.[12,17,38] The sequence of R48-2 peptide is NH-AAGDAGEESRVQVLKNEVRR-COOH (amino acid #16–35; Genemed Synthesis, San Antonio, TX, USA). The TIAF1 (R48-2) antibody was used mainly for IHC and fluorescent immunostaining. Where indicated, this peptide (20 μM) was used to absorb the produced TIAF1(R48-2) antibody (1 μl) in negative control experiments for IHC and fluorescent immunostaining.[36] Also, we generated antibody TIAF1-R48-1 (amino acid #44–60; NH-VEQAYVDKCVCGPSA-COOH) in rabbits, as described.[12] The following specific antibodies used were against: Aβ (MCA2172, AbD/Serotec, Kidlington, UK),[11] APP (MAB348, Chemicon/Millipore, Temecula, CA, USA),[11] Smad4[11] (Santa Cruz Laboratory, Santa Cruz, CA, USA), α tubulin (Sigma) and TIAF1 (Abcam).[11] Fluoro-Jade C (Millipore, Billerica, MA, USA) was used to stain degenerating neurons. Adobe Photoshop CS5 software was used to analyze the extent of protein expression from western blots.

cDNA expression constructs and FRET. TIAF1si, scrambled RNA and stable L929 cell transfectants were prepared as previously described.[5,7] TIAF1 and Smad4 were tagged with enhanced green fluorescence protein (EGFP; in pEGFP-C1, Clontech, Mountain View, CA, USA), ECFP in pECFP-C1 (Clontech) or DsRed in pDsRed (Clontech).[5,7,17] These are mammalian expression plasmids. Additional mammalian expression plasmids were WOX1, p53, dominant-negative TIAF1 (E22/23A), dnJNK1 and dnWOX1.[7,12,17] Where indicated, L929, MCF7, NCI-H1299 cells or other indicated cells were electroporated with the above constructs (200 V, 50 msec; Square Wave BTX ECM830, Genetronics, San Diego, CA, USA), cultured overnight and then treated with TGF-β1 for indicated times. Alternatively, the cells were transfected with the aforementioned DNA constructs using liposome-based Genefector (Venn Nova). Whole cell lysates were prepared in the presence of a cocktail of protease inhibitors (Sigma). The extent of protein expression was determined using indicated specific antibodies in each indicated experiment. FRET analysis for bimolecular interactions was carried out as described.[11,17,35] Briefly, cells were stimulated with an excitation wavelength of 440 nm. FRET signals were detected at an emission wavelength of 535 nm. ECFP and EYFP were used as donor and acceptor fluorescent molecules, respectively. The FRET images were corrected for background fluorescence from an area free of cells. The spectrally corrected FRET concentration (FRETc) was calculated using a software program (Image-Pro Plus 6.1, Media Cybernetics, Bethesda, MD, USA) using Youvan's equation:

$$\mathrm{FRETc} = (\mathrm{fretbk}[\mathrm{fret}]) - \mathrm{cf}[\mathrm{don}] \times (\mathrm{don} - \mathrm{bk}[\mathrm{don}]) - \mathrm{cf}[\mathrm{acc}] \times (\mathrm{acc} - \mathrm{bk}[\mathrm{acc}]),$$

where fret = fret image, bk = background, cf = correction factor, don = donor image and acc = acceptor image. The equation normalizes the FRET signals to the expression levels of the fluorescent proteins.

Quantification of fluorescent images. Fluorescent or immunofluorescent microscopy was performed using a NIKON TE2000-U microscope (Nikon, Tokyo, Japan), as described.[11,17,35,39] For prostate cancer tissue microarray slides, the relative extent of protein expression in each section was quantified

using the histogram tool of the Nikon's EIS Elements BR3.2 software (Nikon). Each slide was quantified independently by two laboratory researchers. For cultured cell images, the relative fluorescence intensities of whole cells or individual punctates were quantified by Photoshop (under the Histogram and Marquee or Quick Selection tools, Adobe Photoshop CS5) and by Nikon's software. For each control or experiment, 20–100 cells were examined in 3–5 experiments. Presented data were from analyses by Photoshop.

Cell proliferation assay and flow cytometry. MTS tetrazolium assay (CellTiter 96 AQueous OneSolution Cell Proliferation Assay, Promega, Madison, WI, USA) was used to measure the extent of cell and colony growth.[7] In addition, cells were transfected with the TIAF1 or indicated constructs by electroporation and cultured for 24–48 h, followed by determining the extent of apoptosis and growth suppression by cell cycle analysis using a fluorescence-activated cell sorting/flow cytometry machine (BD, Sparks, MD, USA), as described.[7,39]

UVB irradiation on hairless mouse skin. The *in vivo* experiments were performed, as described.[15] An approved protocol for animal use was obtained from the Institutional Animal Care and Use Committee of the National Cheng Kung University Medical College. Briefly, hairless SKH-hr1 female mice, 6-week-old, were obtained from Charles River Laboratories (Wilmington, MA, USA). The mice were housed in individual cages in a room with a constant temperature and humidity and an alternating 12-h light and dark cycle, and fed *ad libitum* with a commercial diet and water. To examine acute response, three mice were exposed to UVB (2.16 kJ/m^2; 312 nm) once using a BLE-8T312 UV lamp (Spectronics, Westbury, NY, USA), and the mice were killed 1 day later. To determine chronic response, mice were exposed to UVB thrice per week (Monday, Wednesday and Friday) starting with 0.36 kJ/m^2, respectively, for 1 and 5 months ($n = 3$), followed by increasing 100% weekly. After week 10, a consistent dose of UVB irradiation (2.16 kJ/m^2) was given over the next 8 weeks. In a control group, mice received no UVB irradiation. Skin tissue sections were prepared[15] and processed for IHC staining using TIAF1(R48-2) antibody.

Cell migration or wound healing assay. Cell lines, including breast MDA-MB-231 and MCF cells and murine L929 fibroblasts, were transiently transfected with expression constructs for p53, TIAF1 and/or WOX1 cDNA by electroporation.[5,12,17] Cell migration assay was performed by using Culture-Inserts (ibidi, Verona, WI, USA) in the petridishes, as described.[40] A culture insert was placed on a 35-mm dish, and an equal number of cells (2.8×10^4 cells in 70 μl RPMI or DMEM medium) were seeded into the two reservoirs of the same insert, so as to generate a 500 ± 50 μM gap between two cell populations. After 24-h incubation at 37 °C with 5% CO_2, the insert was gently removed and the medium was removed. Migration experiments were then conducted under serum-free medium. The extent of cell migration was imaged for indicated times using the NIKON TE2000-U microscope.[17,39]

Data analysis. All experiments indicated above were performed 2–5 times. Data were presented as mean ± S.D. Student's *t*-tests were performed for statistical analysis where indicated.

Conflict of Interest

The authors declare no conflict of interest.

Acknowledgements. This research was supported, in part, by the Department of Defense USA (DAMD17-03-1-0736 and W81XWH-08-1-0682), the Guthrie Foundation for Education and Research the National Science Council, Taiwan, ROC (NSC96-2320-B-006-014, 98-2628-B-006-045-MY3, 98-2628-B-006-041-MY3, and 99-2320-B-006-012-MY3), the National Health Research Institute, Taiwan, ROC (NHRI-EX99-9704BI), the National Cheng Kung University Landmark Projects (C0167) and the Department of Health, Taiwan, ROC (DOH101-TD-PB-111-TM010) (to NS Chang). Technical assistance of Jane CY Lu is appreciated.

Author Contributions

MFC, FJL, HMS and CIS provided IRB-approved clinical samples. JYC, SJC, CCH and THH carried out immunohistochemistry. MHL and LYY made DNA constructs. JYC, SRL, MHL, HH, PYC, YAC, and NSC performed experiments. NSC conceived the project, designed experiments, performed imaging analyses, analyzed data and wrote the manuscript. YAC, PYC, HH, FJL, CIS and NSC proofread the manuscript.

1. Wahl SM, Wen J, Moutsopoulos N. TGF-beta: a mobile purveyor of immune privilege. *Immunol Rev* 2006; **213**: 213–227.
2. Mantel PY, Schmidt-Weber CB. Transforming growth factor-beta: recent advances on its role in immune tolerance. *Methods Mol Biol* 2011; **677**: 303–338.
3. Meulmeester E, Ten Dijke P. The dynamic roles of TGF-β in cancer. *J Pathol* 2011; **223**: 205–218.
4. Tian M, Neil JR, Schiemann WP. Transforming growth factor-β and the hallmarks of cancer. *Cell Signal* 2011; **23**: 951–962.
5. Chang NS, Mattison J, Cao H, Pratt N, Zhao Y, Lee C. Cloning and characterization of a novel transforming growth factor-β1-induced TIAF1 protein that inhibits tumor necrosis factor cytotoxicity. *Biochem Biophys Res Commun* 1998; **253**: 743–749.
6. Khera S, Chang NS. TIAF1 participates in the transforming growth factor β1-mediated growth regulation. *Ann NY Acad Sci* 2003; **995**: 11–21.
7. Schultz L, Khera S, Sleve D, Heath J, Chang NS. TIAF1 and p53 functionally interact in mediating apoptosis and silencing of TIAF1 abolishes nuclear translocation of serine 15-phosphorylated p53. *DNA Cell Biol* 2004; **23**: 67–74.
8. van der Leij J, van den Berg A, Albrecht EW, Blokzijl T, Roozendaal R, Gouw AS *et al.* High expression of TIAF-1 in chronic kidney and liver allograft rejection and in activated T helper cells. *Transplantation* 2003; **75**: 2076–2082.
9. Pfoertner S, Jeron A, Probst-Kepper M, Guzman CA, Hansen W, Westendorf AM *et al.* Signatures of human regulatory T cells: an encounter with old friends and new players. *Genome Biol* 2006; **7**: R54.
10. Griseri P, Vos Y, Giorda R, Gimelli S, Beri S, Santamaria G *et al.* Complex pathogenesis of Hirschsprung's disease in a patient with hydrocephalus, vesico-ureteral reflux and a balanced translocation t(3;17)(p12;q11). *Eur J Hum Genet* 2009; **17**: 483–490.
11. Lee MH, Lin SR, Chang JY, Schultz L, Heath J, Hsu LJ *et al.* TGF-β induces TIAF1 self-aggregation via type II receptor-independent signaling that leads to generation of amyloid β plaques in Alzheimer's disease. *Cell Death Dis* 2010; **1**: e110.
12. Chang NS, Pratt N, Heath J, Schultz L, Sleve D, Carey GB *et al.* Hyaluronidase induction of a WW domain-containing oxidoreductase that enhances tumor necrosis factor cytotoxicity. *J Biol Chem* 2001; **276**: 3361–3370.
13. Chang NS, Hsu LJ, Lin YS, Lai FJ, Sheu HM.. WW domain-containing oxidoreductase: a candidate tumor suppressor. *Trends Mol Med* 2007; **13**: 12–22.
14. Chang JY, He RY, Lin HP, Hsu LJ, Lai FJ, Hong Q *et al.* Signaling from membrane receptors to tumor suppressor WW domain-containing oxidoreductase. *Exp Biol Med* 2010; **235**: 796–804.
15. Lai FJ, Cheng CL, Chen ST, Wu CH, Hsu LJ, Lee JY *et al.* WOX1 is essential for UVB irradiation-induced apoptosis and down-regulated via translational blockade in UVB-induced cutaneous squamous cell carcinoma in vivo. *Clin Cancer Res* 2005; **11**: 5769–5777.
16. Chang NS, Joki N, Mattison J, Dinh T, John S.. Characterization of serum adhesive proteins that block tumor necrosis factor-mediated cell death. *Cell Death Differ* 1997; **4**: 779–786.
17. Hsu LJ, Schultz L, Hong Q, Van Moer K, Heath J, Li MY *et al.* Transforming growth factor beta1 signaling via interaction with cell surface Hyal-2 and recruitment of WWOX/WOX1 *J Biol Chem* 2009; **284**: 16049–16059.
18. Bykov VJ, Selivanova G, Wiman KG. Small molecules that reactivate mutant p53 *Eur J Cancer* 2003; **39**: 1828–1834.
19. Chang NS. Hyaluronidase activation of c-Jun N-terminal kinase is necessary for protection of L929 fibrosarcoma cells from staurosporine-mediated cell death. *Biochem Biophys Res Commun* 2001; **283**: 278–826.
20. Hong Q, Hsu LJ, Schultz L, Pratt N, Mattison J, Chang NS.. Zfra affects TNF-mediated cell death by interacting with death domain protein TRADD and negatively regulates the activation of NF-kappaB, JNK1, p53 and WOX1 during stress response. *BMC Mol Biol* 2007; **8**: 50.
21. Di Fiore F, Sesboüé R, Michel P, Sabourin JC, Frebourg T. Molecular determinants of anti-EGFR sensitivity and resistance in metastatic colorectal cancer. *Br J Cancer* 2010; **103**: 1765–1772.
22. Fröhlich E. Proteases in cutaneous malignant melanoma: relevance as biomarker and therapeutic target. *Cell Mol Life Sci* 2010; **67**: 3947–3960.
23. Golubovskaya VM, Cance W. Focal adhesion kinase and p53 signal transduction pathways in cancer. *Front Biosci* 2010; **15**: 901–912.
24. Taylor MA, Parvani JG, Schiemann WP. The pathophysiology of epithelial-mesenchymal transition induced by transforming growth factor-beta in normal and malignant mammary epithelial cells. *J Mammary Gland Biol Neoplasia* 2010; **15**: 169–190.
25. Simpson MA, Lokeshwar VB. Hyaluronan and hyaluronidase in genitourinary tumors. *Front Biosci* 2008; **13**: 5664–5680.

26. Perera M, Tsang CS, Distel RJ, Lacy JN, Ohno-Machado L, Ricchiuti V *et al.* TGF-beta1 interactome: metastasis and beyond. *Cancer Genomics Proteomics* 2010; **7**: 217–229.
27. Kraljevic Pavelic S, Sedic M, Bosnjak H, Spaventi S, Pavelic K. Metastasis: new perspectives on an old problem. *Mol Cancer* 2011; **10**: 22.
28. Schaller BJ, Buchfelder M. Neuroprotection in primary brain tumors: sense or nonsense? *Expert Rev Neurother* 2006; **6**: 723–730.
29. Stern R. Association between cancer and "acid mucopolysaccharides": an old concept comes of age, finally. *Semin Cancer Biol* 2008; **18**: 238–243.
30. Mao R, Fan Y, Mou Y, Zhang H, Fu S, Yang J. TAK1 lysine 158 is required for TGF-β-induced TRAF6-mediated Smad-independent IKK/NF-κB and JNK/AP-1 activation. *Cell Signal* 2011; **23**: 222–227.
31. Cordray P, Satterwhite DJ. TGF-beta induces novel Lef-1 splice variants through a Smad-independent signaling pathway. *Dev Dyn* 2005; **232**: 969–978.
32. Droguett R, Cabello-Verrugio C, Satander C, Brandan E. TGF-beta receptors, in a Smad-independent manner, are required for terminal skeletal muscle differentiation. *Exp Cell Res* 2010; **316**: 2487–2503.
33. Watanabe A, Hippo Y, Taniguchi H, Iwanari H, Yashiro M, Hirakawa K *et al.* An opposing view on WWOX protein function as a tumor suppressor. *Cancer Res* 2003; **63**: 8629–8633.
34. Chang NS, Schultz L, Hsu LJ, Lewis J, Su M, Sze CI. 17beta-estradiol upregulates and activates WOX1/WWOXv1 and WOX2/WWOXv2 *in vitro*: potential role in cancerous progression of breast and prostate to a premetastatic state *in vivo*. *Oncogene* 2005; **24**: 714–723.
35. Li MY, Lai FJ, Hsu LJ, Lo CP, Cheng CL, Lin SR *et al.* Dramatic co-activation of WWOX/WOX1 with CREB and NF-kappaB in delayed loss of small dorsal root ganglion neurons upon sciatic nerve transection in rats. *PLoS One* 2009; **4**: e7820.
36. Chen ST, Chuang JI, Cheng CL, Hsu LJ, Chang NS. Light-induced retinal damage involves tyrosine 33 phosphorylation, mitochondrial and nuclear translocation of WW domain-containing oxidoreductase *in vivo*. *Neuroscience* 2005; **130**: 397–407.
37. Oliveira VC, Carrara RC, Simoes DL, Saggioro FP, Carlotti CG Jr, Covas DT *et al.* Sudan Black B treatment reduces autofluorescence and improves resolution of in situ hybridization specific fluorescent signals of brain sections. *Histol Histopathol* 2010; **25**: 1017–1024.
38. Sze CI, Su M, Pugazhenthi S, Jambal P, Hsu LJ, Heath J *et al.* Down-regulation of WW domain-containing oxidoreductase induces Tau phosphorylation in vitro. A potential role in Alzheimer's disease. *J Biol Chem* 2004; **279**: 30498–30506.
39. Lin HP, Chang JY, Huang SS, Lin SR, Lee MH, Hsu LJ *et al.* Phorbol ester dissociates an *in vivo* MEK/WOX1 complex for switching on a novel type of apoptosis in T lymphocytes. *Genes Cancer* 2011; **2**: 550.
40. Goyal P, Behring A, Kumar A, Siess W. STK35L1 associates with nuclear actin and regulates cell cycle and migration of endothelial cells. *PLoS One* 2011; **6**: e16249.

Supplementary Information accompanies the paper on Cell Death and Disease website (http://www.nature.com/cddis)